ruhr.paD
UA Ruhr Zentrum für
partielle Differentialgleichungen

L^1 penalization of volumetric dose objectives in optimal control of PDEs

R.C. Barnard and Ch. Clason

Preprint 2016-04

L^1 penalization of volumetric dose objectives in optimal control of PDEs*

Richard C. Barnard† Christian Clason‡

July 6, 2016

This work is concerned with a class of optimal control problems governed by a partial differential equation that are motivated by an application in radiotherapy treatment planning, where the primary design objective is to minimize the volume where a functional of the state violates a prescribed level, but prescribing these levels in the form of pointwise state constraints can lead to infeasible problems. We therefore propose an alternative approach based on L^1 penalization of the violation. We establish well-posedness of the corresponding optimal control problem, derive first-order optimality conditions, and present a semismooth Newton method for the efficient numerical solution of these problems. The performance of this method for a model problem is illustrated and contrasted with the alternative approach based on (regularized) state constraints.

1 Introduction

We consider optimal control problems governed by linear partial differential equations in which the region where the state is greater than or less than a prescribed level is to be minimized. Such problems arise in radiotherapy treatment planning, where the aim is to deposit a radiative dose sufficiently strong to destroy tumor tissue while also minimizing damage to nearby healthy organs and structures. Specifically, on the target region (the tumor) we wish the *accumulated* output of the system to exceed a prescribed level U, while on the risk region (the healthy organs), we wish the accumulated output to not exceed a prescribed level L. Due to the usual

*This manuscript has been authored by UT-Battelle, LLC, under Contract No. DE-AC0500OR22725 with the U.S. Department of Energy. The United States Government retains and the publisher, by accepting the article for publication, acknowledges that the United States Government retains a non-exclusive, paid-up, irrevocable, world-wide license to publish or reproduce the published form of this manuscript, or allow others to do so, for the United States Government purposes. The Department of Energy will provide public access to these results of federally sponsored research in accordance with the DOE Public Access Plan (http://energy.gov/downloads/doe-public-access-plan).

†Oak Ridge National Laboratory, Oak Ridge, TN 37831, USA (barnardrc@ornl.gov)

‡Faculty of Mathematics, University Duisburg-Essen, 45117 Essen, Germany (christian.clason@uni-due.de)

close proximity of tumors and healthy organs, it is usually not possible to satisfy these constraints over the whole region. Since a successful therapy only requires destroying (i.e., depositing a dose exceeding U) a sufficiently large part of the tumor, and healthy organs remain viable if a sufficiently large part remains undamaged (i.e., has a dose below L), volumetric conditions are used in evaluating structure survival probabilities. These are usually given in the form of dose volume histograms (DVH); see, e.g., [16].

Such performance criteria would be well-captured by an L^0 penalty on the violation of the prescribed limits. However, in light of well-established difficulties associated with L^0 minimization, we instead use L^1 penalty terms. Specifically, let $\Omega \subset \mathbb{R}^n$ be given and let $\omega_T, \omega_R \subset \Omega$ bounded and disjoint be a target region and a risk region, respectively. Let $\mathcal{E}(y,u) = 0$ denote the partial differential equation with $\mathcal{E} : W \times V \to Y$ (for suitable Hilbert spaces W, V, Y) and let $C_\omega : L^2(0,T;L^1(\omega)) \to L^1(\omega)$ (for either $\omega = \omega_R$ or $\omega = \omega_T$) denote the integral operator $y(t,x) \mapsto \int_0^T \chi_\omega(x) y(t,x)\,dt$. For the sake of generality, we also include a quadratic tracking term with respect to a desired state $z \in L^2(Q) := L^2(0,T;L^2(\Omega))$. We then consider problems of the form

$$\begin{cases} \min\limits_{u\in V_{\text{ad}},\ y\in Y} \dfrac{1}{2}\|u\|_V^2 + \dfrac{\alpha}{2}\|y-z\|_{L^2(Q)}^2 + \beta_1\|(C_{\omega_T}y - U)^-\|_{L^1(\omega_T)} + \beta_2\|(C_{\omega_R}y - L)^+\|_{L^1(\omega_R)} \\ \quad \text{s.t.} \quad \mathcal{E}(y,u) = 0, \end{cases} \tag{1.1}$$

where $\alpha \geq 0$ and $\beta_1, \beta_2 > 0$, $(u)^+ = \max\{0,u\}$ and $(u)^- = \min\{0,u\}$ pointwise almost everywhere, $0 < L < U$, and $V_{\text{ad}} \subset V$ is a set of admissible controls to be specified below. (Spatially varying levels U and L are possible as well.) We call the addition of these L^1-penalty terms a *volumetric dose penalization*, in keeping with the motivational problem from radiotherapy treatment planning. For the sake of illustration, we consider in this paper as a model equation

$$\mathcal{E}(y,u) = y_t - c\Delta y - E_{\omega_C}u \tag{1.2}$$

for some $c > 0$ together with initial conditions $y(0) = y_0 \in L^2(\Omega)$ and homogeneous Dirichlet boundary conditions, where $E_{\omega_C} : V := L^2(0,T;L^2(\omega_C)) \to L^2(0,T;L^2(\Omega))$ denotes the extension by zero operator and $\omega_C \subset \Omega$ is the bounded control region. However, the subsequent analysis holds for more general linear PDEs. We also note that the analysis in the following sections can be extended to problems where C_ω takes the form of some other bounded, linear functional.

As an alternative approach, one could attempt to achieve the design objectives listed above by way of pointwise state constraints on the target and risk region, i.e., by considering

$$\begin{cases} \min\limits_{u\in V_{\text{ad}},\ y\in Y} \dfrac{1}{2}\|u\|_V^2 + \dfrac{\alpha}{2}\|y-z\|_{L^2(Q)}^2 \\ \quad \text{s.t.} \quad \mathcal{E}(y,u) = 0, \\ \qquad\ \ C_{\omega_T}y \geq U \quad \text{a.e. in } \omega_T, \\ \qquad\ \ C_{\omega_R}y \leq L \quad \text{a.e. in } \omega_R. \end{cases} \tag{1.3}$$

However, since the observed dose $C_\omega y$ is continuous and $L < U$, this problem is not well-posed due to the absence of feasible points if ω_T and ω_R are not separated by a strictly positive distance;

as tumors can (and frequently will) occur inside vital organs, this separation does not hold in practice. (We point out that any conforming discretization of the problem will also have no feasible points.) For instance, even in simple academic problems as in [1], deploying a sufficient radiative dose on the tumor is impossible unless high levels of dose are also placed on at least some portion the healthy tissue. This becomes even more clear when additional constraints on the control are included, such as requiring the control to be a beam of a certain shape or direction. On the other hand, if we modify the problem so that the sets are open and disjoint, the reduced cost functional for the continuous problem will not be weakly lower semicontinuous. If one takes a cavalier approach and attempts to numerically solve the problem using, e.g., the method in [14], one will tend to run into a numerical locking as seen in the examples below. In contrast, (1.1) suffers from no such difficulty in these situations; while of course we can not expect a solution which is feasible for (1.3), the theoretical existence and uniqueness of solutions is still assured and we shall see that the numerical performance is still reasonable. In particular, we stress that (1.1) should not be interpreted as an exact penalization of (1.3).

Let us briefly comment on related literature. A fully discretized formulation of the radiotherapy treatment planning problem as a convex linear-quadratic program was studied in [17]. A treatment strategy using convexified DVH constraints was considered in [21]. However in these two works, the physics of dose deposition are discretized using precomputed beamlets; this simplification gives significant errors in dose calculation [19]. Regarding radiotherapy planning and its formulation as a pde-constrained optimization problem, we refer to, e.g., [1, 9, 10], which use physically accurate models but do not treat DVH-based optimization strategies. Additionally, such models involve a significant increase in computational costs, meaning efficient optimization methods in the context of pde-constrained problems are needed. Regarding L^1-minimization, its application to partial differential equations was first considered in the context of sparse control; see, e.g., [18, 11]. L^1 penalization of other constraints in optimal control of pdes was treated in [6, 4, 7].

This work is organized as follows. In Section 2, we establish the well-posedness of (1.1) and derive necessary optimality conditions. We then turn in Section 3 to the issue of the numerical solutions of (1.1) via Moreau–Yosida regularization, which allows for the use of a superlinearly convergent semismooth Newton method. Numerical examples illustrating the behavior of the proposed approach are presented in Section 4.

2 Existence and optimality conditions

We first formulate (1.1) in reduced form. Let $V := L^2(0,T;L^2(\omega_C))$,

$$V_{\text{ad}} := \left\{ u \in L^2(0,T;L^2(\omega_C)) : U_{\min} \le u(x) \le U_{\max} \text{ for a.e. } x \in \omega_C \right\}$$

denote the admissible control set and set

$$W := L^2(0,T;H_0^1(\Omega)) \cap H^1(0,T;H^{-1}(\Omega) \hookrightarrow Y := L^2(0,T;L^2(\Omega)).$$

By the well-posedness of (1.2), we can introduce a control-to-state mapping

$$S : V_{\text{ad}} \to Y, \qquad u \mapsto y \quad \text{solving} \quad y_t - c\Delta y = E_{\omega_C} u, \quad y(0) = y_0, \quad y|_{\partial\Omega} = 0.$$

We make the assumption that the range of S embeds compactly into $L^p(0,T;L^p(\Omega))$ for some $p > 2$. This implies that S is completely continuous, i.e., $u_n \rightharpoonup u$ in V implies $Su_n \to Su$ in Y. Furthermore, since S is affine, its Fréchet derivative $S' =: S_0$ is given by the solution of (1.2) with homogeneous initial conditions. We assume that its adjoint S_0^* satisfies the same range assumption as S. We also note for future use that these assumptions imply that the range of $C_\omega S$ is contained in $L^p(\omega)$ for any subdomain $\omega \subset \Omega$.

We can thus formulate the reduced problem

$$(\mathcal{P}) \qquad \min_{u \in V_{\mathrm{ad}}} \frac{1}{2}\|u\|_V^2 + \frac{\alpha}{2}\|Su - z\|_{L^2(Q)}^2 + \beta_1 \|(C_{\omega_T} Su - U)^-\|_{L^1(\omega_T)} + \beta_2 \|(C_{\omega_R} Su - L)^+\|_{L^1(\omega_R)}.$$

The final two terms take the form of integrals of convex and Lipschitz continuous integrands $g^+, g^- : \mathbb{R} \to \mathbb{R}$ with

$$g^+(v) := |(v-L)^+| = \begin{cases} 0 & v \le L, \\ v - L & v \ge L, \end{cases} \qquad g^-(v) := |(v-U)^-| = \begin{cases} U - v & v \le U, \\ 0 & v \ge U. \end{cases}$$

Since the bounded operators C and S are, respectively, linear and affine, the cost function is the sum of convex and weakly lower semicontinuous functionals, and we obtain existence of an optimal control by Tonelli's direct method. Due to the strictly convex control cost term, the optimal control is unique.

Theorem 2.1. *There exists a unique minimizer $\bar{u} \in V_{ad}$ to $(\mathcal{P})$.*

To derive optimality conditions, we apply the sum and chain rules of convex analysis. We first compute the subdifferentials of the volumetric dose penalty terms via the subdifferentials of the corresponding integrands g^+, g^-. Since both functions can be written as the maximum of two convex and differentiable functions, their convex subdifferential is given pointwise by the convex hull of the derivatives of the active functions (see, e.g., [13, Corollary 4.3.2]), i.e.,

$$\partial g^+(v) = \begin{cases} \{0\} & v < L, \\ \{1\} & v > L, \\ [0,1] & v = L, \end{cases} \qquad \partial g^-(v) = \begin{cases} \{-1\} & v < U, \\ \{0\} & v > U, \\ [-1,0] & v = U. \end{cases} \tag{2.1}$$

We also introduce the indicator function $\delta_{V_{\mathrm{ad}}} : L^2(0,T;L^2(\omega_C)) \to \overline{\mathbb{R}}$ in the sense of convex analysis, i.e., $\delta_{V_{\mathrm{ad}}}(u) = 0$ if $u \in V_{\mathrm{ad}}$ and $\delta_{V_{\mathrm{ad}}}(u) = \infty$ else. Finally, set

$$G^+ : L^2(\omega_R) \to \mathbb{R}, \qquad y \mapsto \int_{\omega_R} g^+(y(x))\,dx$$

and similarly for $G^- : L^2(\omega_T) \to \mathbb{R}$. We then obtain the following optimality conditions.

Theorem 2.2. *Let $\bar{u} \in V_{ad}$ be a minimizer of $(\mathcal{P})$. Then there exist $\bar{\mu}^+ \in L^2(\omega_R)$ and $\bar{\mu}^- \in L^2(\omega_T)$ such that*

$$\text{(OS)} \qquad \begin{cases} \bar{u} = \mathrm{proj}_{V_{ad}}\left(-S_0^*\left(\alpha(S\bar{u} - z) + \beta_1 C_{\omega_R}^* \bar{\mu}^+ + \beta_2 C_{\omega_T}^* \bar{\mu}^-\right)\right), \\ \bar{\mu}^+(x) \in \partial g^+([C_{\omega_R} S\bar{u}](x)) \quad \text{for a.e. } x \in \omega_R, \\ \bar{\mu}^-(x) \in \partial g^-([C_{\omega_T} S\bar{u}](x)) \quad \text{for a.e. } x \in \omega_T. \end{cases}$$

Proof. Since ($\mathcal{P}$) is convex, S and C_ω are continuous, and all terms apart from the indicator function are finite-valued, the sum and chain rules of convex analysis (see, e.g., [8, Prop. I.5.6, Prop. I.5.7]) yield the necessary optimality conditions

$$0 \in \{\bar{u}\} + \{\alpha S_0^*(S\bar{u} - z)\} + \beta_1 C_{\omega_T}^* S_0^* \partial G^-(C_{\omega_T} S\bar{u}) + \beta_2 C_{\omega_R}^* S_0^* \partial G^+(C_{\omega_R} S\bar{u}) + \partial \delta_{V_{\mathrm{ad}}}(\bar{u}).$$

The fact that the subdifferential of the convex integral functional G^+ and G^- can be computed pointwise (see, e.g. [2, Prop. 16.50]) yields the second and third relation of (OS). Rearranging the remaining terms yields

$$-\bar{u} - S_0^* \left(\alpha(S\bar{u} - z) + \beta_1 C_{\omega_R}^* \bar{\mu}^+ + \beta_2 C_{\omega_T}^* \bar{\mu}^- \right) \in \partial \delta_{V_{\mathrm{ad}}}(\bar{u}),$$

which can be reformulated (denoting the second term on the left hand side by $\bar{p}$ for brevity)

$$\begin{aligned} -\bar{u} + \bar{p} \in \partial \delta_{V_{\mathrm{ad}}}(\bar{u}) &\Leftrightarrow \bar{p} \in \{\bar{u}\} + \partial \delta_{V_{\mathrm{ad}}}(\bar{u}) \\ &\Leftrightarrow \bar{u} \in (\mathrm{Id} + \partial \delta_{V_{\mathrm{ad}}})^{-1}(\bar{p}) = \mathrm{proj}_{V_{\mathrm{ad}}}(\bar{p}), \end{aligned}$$

using the fact that the resolvent of an indicator function of a convex set coincides with the (single-valued) metric projection onto this set; cf., e.g., [2, Ex. 12.25]. This gives the first relation of (OS). □

3 Numerical solution

In order to solve (OS_γ), we proceed similarly to [5] and use a semismooth Newton method applied to a Moreau–Yosida regularization of (OS).

3.1 Moreau–Yosida regularization

To compute the Moreau–Yosida regularization, we replace ∂g^+ for $\gamma > 0$ by

$$\partial g_\gamma^+(v) := (\partial g^+)_\gamma(v) := \frac{1}{\gamma} \left(v - \mathrm{prox}_{\gamma g^+}(v) \right),$$

where

$$\mathrm{prox}_{\gamma g^+}(v) := \arg\min_{w \in \mathbb{R}} \frac{1}{2\gamma} |w - v|^2 + g^+(w) = (\mathrm{Id} + \gamma \partial g^+)^{-1}(v)$$

is the proximal mapping of g^+, which in Hilbert spaces coincides with the resolvent of ∂g^+; see, e.g., [2, Prop. 16.34]. Note that the proximal mapping and thus the Moreau–Yosida regularization of a proper and convex functional is always single-valued and Lipschitz continuous; see, e.g., [2, Corollary 23.10].

We begin by calculating the proximal mapping of g^+, proceeding as in [4]. For given $\gamma > 0$ and $v \in \mathbb{R}$, the resolvent $w := (\mathrm{Id} + \gamma \partial g^+)^{-1}(v)$ is characterized by the subdifferential inclusion

$$v \in (\mathrm{Id} + \gamma \partial g^+)(w) = \{w\} + \gamma \partial g^+(w).$$

We now follow the case discrimination in the characterization (2.1) of the subdifferential.

(i) $w < L$: In this case, we have that $v = w < L$.

(ii) $w > L$: In this case, we have that $v = w + \gamma < L + \gamma$, i.e., $w = v - \gamma$.

(iii) $w = L$: In this case, we have that $v \in w + \gamma[0,1] = [L, L + \gamma]$.

Since these cases yield a complete and disjoint case distinction for v, we obtain

$$\operatorname{prox}_{\gamma g^+}(v) = \begin{cases} v & \text{if } v < L \\ L & \text{if } v \in [L, L+\gamma], \\ v - \gamma & \text{if } v > L + \gamma. \end{cases}$$

Inserting this into the definition of the Moreau–Yosida regularization gives

$$\partial g_\gamma^+(v) = \begin{cases} 0 & \text{if } v < L \\ \frac{1}{\gamma}(v - L) & \text{if } v \in [L, L+\gamma], \\ 1 & \text{if } v > L + \gamma. \end{cases}$$

Proceeding similarly for g^-, we find that

$$\operatorname{prox}_{\gamma g^-}(v) = \begin{cases} v + \gamma & \text{if } v < U - \gamma \\ U & \text{if } v \in [U - \gamma, U], \\ v & \text{if } v > U, \end{cases}$$

and hence

$$\partial g_\gamma^-(v) = \begin{cases} -1 & \text{if } v < U - \gamma \\ \frac{1}{\gamma}(v - U) & \text{if } v \in [U - \gamma, U], \\ 0 & \text{if } v > U. \end{cases}$$

Replacing the subdifferentials with their regularizations in (OS), we arrive at the regularized system

$$(\mathrm{OS}_\gamma) \qquad \begin{cases} u_\gamma = \operatorname{proj}_{V_{\mathrm{ad}}}\left(-S_0^*\left(\alpha(Su_\gamma - z) + \beta_1 C_{\omega_R}^* \mu_\gamma^+ + \beta_2 C_{\omega_T}^* \mu_\gamma^-\right)\right), \\ \mu_\gamma^+(x) = \partial g_\gamma^+([C_{\omega_R} S u_\gamma](x)), \\ \mu_\gamma^-(x) = \partial g_\gamma^-([C_{\omega_T} S u_\gamma](x)). \end{cases}$$

Theorem 3.1. *For every $\gamma > 0$, there exists $(u_\gamma, \mu_\gamma^+, \mu_\gamma^+)$ satisfying (OS_γ).*

Proof. We use the fact that $\partial g_\gamma^+(v)$ is the derivative of the (convex and lower semicontinuous) Moreau envelope

$$g_\gamma^+(v) := g^+(\operatorname{prox}_{\gamma g^+}(v)) + \frac{1}{2\gamma}|v - \operatorname{prox}_{\gamma g^+}(v)|^2,$$

see, e.g., [2, Remark 12.24, Proposition 12.29]; a similar statement holds for ∂g_γ^-. Hence, (OS_γ) are the necessary optimality conditions of the convex minimization problem

$$\min_{u\in V_{\mathrm{ad}}} \frac{1}{2}\|u\|_V^2 + \frac{\alpha}{2}\|Su - z\|_{L^2(Q)}^2 + \beta_1 \int_{\omega_T} g_\gamma^-(C_{\omega_T} Su)\,dx + \beta_2 \int_{\omega_T} g_\gamma^+(C_{\omega_R} Su)\,dx,$$

which admits a unique solution. □

Remark 1. *The Moreau envelopes of g^+ and g^- are given by*

$$g_\gamma^+(v) = \begin{cases} 0 & \text{if } v < L, \\ v - L - \frac{\gamma}{2} & \text{if } v > L + \gamma, \\ \frac{1}{2\gamma}(v-L)^2 & \text{if } v \in [L, L+\gamma], \end{cases} \qquad g_\gamma^-(v) = \begin{cases} U - v - \frac{\gamma}{2} & \text{if } v < U - \gamma, \\ 0 & \text{if } v > U, \\ \frac{1}{2\gamma}(v-U)^2 & \text{if } v \in [U-\gamma, U]. \end{cases}$$

The Moreau–Yosida regularization of the dose penalty is thus related to the well-known Huber-regularization of the L^1 norm.

We conclude this section by noting that solutions to the regularized system (OS_γ) converge weakly up to a subsequence to solutions of the original optimality system (OS).

Theorem 3.2. *The family $\{(u_\gamma, \mu_\gamma^+, \mu_\gamma^-)\}_{\gamma>0}$ contains a sequence $\{(u_{\gamma_n}, \mu_{\gamma_n}^+, \mu_{\gamma_n}^-)\}_{n\in\mathbb{N}}$ converging weakly to a solution $(\bar u, \bar\mu^+, \bar\mu^-)$ of (OS).*

Proof. The proof follows largely as in Proposition 2.5 of [4]. We note that for any $u \in V$, $\partial g_\gamma^+(u(x))$ and $\partial g_\gamma^-(u(x))$ are bounded almost everywhere, implying that $\{\mu_\gamma^+\}_{\gamma>0}, \{\mu_\gamma^-\}_{\gamma>0}$ are bounded. As S_0^* and C_ω^* are bounded linear operators, the family

$$\{p_\gamma\}_{\gamma>0} := \left\{ S_0^* \left(\alpha(Su_\gamma - z) + \beta_1 C_{\omega_R}^* \mu_\gamma^+ + \beta_2 C_{\omega_T}^* \mu_\gamma^- \right) \right\}_{\gamma>0}$$

is bounded in V. This in turn implies the boundedness of $\{u_\gamma\}_{\gamma>0}$. Hence there exists a subsequence converging weakly to $(\hat p, \hat u, \hat\mu^+, \hat\mu^-)$. As g^+ and g^- are convex, and therefore $\partial g^+(u(x))$ and $\partial g^-(u(x))$ are maximal monotone for every $u \in V$ and almost every $x \in \omega_C$, we have by [3, Lemma 1.3 (e)] that $\hat\mu^+, \hat\mu^-$ satisfy the second and third relations of (OS). The first relation follows similarly, using that $u = \mathrm{proj}_{V_{\mathrm{ad}}}(p)$ is equivalent to the subdifferential inclusion $-u + p \in \partial\delta_{V_{\mathrm{ad}}}(u)$; see the proof of Theorem 2.2. □

3.2 Semismooth Newton method

The solution to (OS_γ) can be computed using a semismooth Newton method [15, 20]. Since $h_\gamma^+ := \partial g_\gamma^+$ and $h_\gamma^- := \partial g_\gamma^-$ are globally Lipschitz continuous and piecewise differentiable, they are Newton-differentiable with Newton derivatives given by

$$D_N h_\gamma^+(v) = \begin{cases} \frac{1}{\gamma} & \text{if } v \in [L, L+\gamma], \\ 0 & \text{else,} \end{cases} \qquad D_N h_\gamma^-(v) = \begin{cases} \frac{1}{\gamma} & \text{if } v \in [U-\gamma, U], \\ 0 & \text{else,} \end{cases}$$

see, e.g., [20, Proposition 2.26]. Similarly, $\operatorname{proj}_{\{[U_{\min}, U_{\max}]\}}(v)$ is Newton-differentiable with Newton derivative

$$D_N \operatorname{proj}_{\{[U_{\min}, U_{\max}]\}}(v) = \begin{cases} 1 & \text{if } v \in [U_{\min}, U_{\max}], \\ 0 & \text{else.} \end{cases}$$

This implies that the corresponding superposition operators $H_\gamma^\pm : L^p(\omega) \to L^2(\omega)$ as well as $\operatorname{proj}_{V_{\mathrm{ad}}} : L^p(0,T;L^p(\omega_C)) \to L^2(0,T;L^2(\omega_C))$ are semismooth, with Newton derivatives given pointwise by, e.g.,

$$[D_N H_\gamma^+(y)](x) = \frac{1}{\gamma}[\chi^+(y)](x) := \begin{cases} \frac{1}{\gamma} & \text{if } y(x) \in [L, L+\gamma], \\ 0 & \text{else,} \end{cases}$$

and $D_N \operatorname{proj}_{V_{\mathrm{ad}}}(y) = \chi_{V_{\mathrm{ad}}}(y)$; see, e.g., [15, Example 8.12] or [20, Theorem 3.49].

To apply a semismooth Newton to (OS_γ), we rewrite it by eliminating $\mu_\gamma^+, \mu_\gamma^-$ as

$$u_\gamma - \operatorname{proj}_{V_{\mathrm{ad}}}\left(-S_0^*\left(\alpha(Su_\gamma - z) + \beta_1 C_{\omega_R}^* H_\gamma^+(C_{\omega_R} S u_\gamma) + \beta_2 C_{\omega_T}^* H_\gamma^-(C_{\omega_T} S u_\gamma)\right)\right) = 0. \tag{3.1}$$

By the sum and chain rules of Newton derivatives (see, e.g., [20, Theorem 3.69]) as well as the range condition on S and S_0^*, it follows that (3.1)—taken as an operator equation $T(u) = 0$ for $T : L^2(0,T;L^2(\omega_C)) \to L^2(0,T;L^2(\omega_C))$—is semismooth.

In order to establish the invertibility of the Newton step $D_N T(u^k)\delta u = -T(u^k)$, i.e.,

$$\left(\mathrm{Id} + \chi_{V_{\mathrm{ad}}}(-F(u^k)) D_N F(u^k)\right)\delta u = -\left(u^k - \operatorname{proj}_{V_{\mathrm{ad}}}(-F(u^k))\right) \tag{3.2}$$

with

$$\begin{aligned} F(u^k) &:= S_0^*\left(\alpha(Su^k - z) + \beta_1 C_{\omega_R}^* H_\gamma^+(C_{\omega_R} S u^k) + \beta_2 C_{\omega_T}^* H_\gamma^-(C_{\omega_T} S u^k)\right), \\ D_N F(u^k) &= S_0^*\left(\alpha + \tfrac{\beta_1}{\gamma} C_{\omega_R}^* \chi^+(C_{\omega_R} S_0 u^k) C_{\omega_R} + \tfrac{\beta_2}{\gamma} C_{\omega_T}^* \chi^-(C_{\omega_T} S_0 u^k) C_{\omega_T}\right) S_0, \end{aligned}$$

we note that $D_N F(u^k) = S_0^* A S_0$ for a positive and self-adjoint linear operator A, and thus that $D_N F(u^k)$ is positive and self-adjoint for every u^k. We recall the following result:

Lemma 3.3 (Corrected Corollary 3.5 of [11, 12])**.** *If A and B are positive, self-adjoint operators on a Hilbert space, then $\sigma(AB) \subset [0,\infty)$.*

As $\chi_{V_{\mathrm{ad}}}(u^k)$ is positive for any u^k, we have that $\sigma\left(\chi_{V_{\mathrm{ad}}}(u^k) D_N F(u^k)\right) \subset [0,\infty)$ for any $k \in \mathbb{N}$, and therefore $\mathrm{Id} + \chi_{V_{\mathrm{ad}}}(u^k) D_N F(u^k)$ is uniformly invertible.

By standard arguments, the uniform invertibility of the left-hand side operator in (3.2) together with the Newton-differentiability implies local superlinear convergence of the corresponding semismooth Newton method to a solution to (OS_γ) for each $\gamma > 0$; see, e.g., [15, Thm. 8.16], [20, Chap. 3.2].

For given h, the application of the Newton derivative $D_N F(u^k)h$ can be computed by solving the linearized state equation (1.2), applying pointwise operations, and then solving the linearized adjoint equation (which for our model problem coincides with (1.2). Hence, the update δu solving

the semismooth Newton step $D_N T(u^k)\delta u = -T(u^k)$ can be computed by a matrix-free Krylov method. To account for the local convergence of Newton methods, we embed the semismooth Newton method within a homotopy strategy for γ, where we start with a large γ which is successively reduced, taking the previous solution as starting point. Furthermore, we include a backtracking line search based on the residual norm $\|T(u^{k+1})\|$ to improve robustness. Our Python implementation of this approach, which was used to generate the results below, can be downloaded from https://www.github.com/clason/dvhpenalty.

4 Numerical examples

To illustrate the performance of the proposed approach, we compare the effects of the volumetric dose penalty with the corresponding state constraints for a simple model problem. Let $\Omega = [-1, 1]$, $T = 1$, and $c = 0.01$. We choose the tumor, risk and control regions as $\omega_T := [-0.45, 0.45] \setminus [-0.2, 0.2]$, $\omega_R := [-0.7, -0.55] \cup [0.55, 0.7] \cup [-0.2, 0.2]$, and $\omega_C = \Omega$, respectively. We further let $U = 0.5$, $L = 0.2$ and $V_{\text{ad}} = \{u \in L^2(0, T; L^2(\omega_C)) : u \geq 0\}$. Finally, we set $\alpha = 0$ and accordingly do not require a target z. To illustrate the influence of the dose penalty parameters β_1 (on the tumor) and β_2 (on the risk region), we set $\beta_1 = \tilde{\beta}_1 |\omega_T|^{-1}$ and $\beta_2 = \tilde{\beta}_2 |\omega_R|^{-1}$ for $\tilde{\beta}_1, \tilde{\beta}_2 \in \{10^3, 10^4\}$, where $|\omega_T| = 0.5$ and $|\omega_R| = 0.7$ denote the Lebesgue measure of the tumor and risk region, respectively; this scaling ensures that if $\tilde{\beta}_1 = \tilde{\beta}_2$, both objectives are given equal weight. We also solve (1.3) with identical parameters (where applicable) by solving a sequence of Moreau–Yosida-regularized problems (which coincide with a quadratic penalization of the state constraints with penalty parameter γ^{-1}) via a semismooth Newton method as outlined in [14].

In the following, a spatial discretization with 256 nodes and 256 time steps are used. In order to compute for each γ a minimizer of the Moreau–Yoshida regularization of (1.1) and (1.3), we use a maximum of 100 semismooth Newton iterations; each Newton step is computed using GMRES with a maximum of 3000 iterations. We initialize γ as 10^2 for (1.1) and as 1 for (1.3), and in both cases reduce γ by a factor of 2 as long as the Newton method converges until γ reaches 10^{-7}. The convergence criterion used for the Newton iterations is a reduction to below 10^{-6} of the norm of the optimality system. The results for solving (1.3) and (1.1) are given in Figure 1 and Figures 2–5, respectively, for the last value of γ (noted below) for which the semismooth Newton method converged. In each case, the dose volume histogram shows the fraction of the area of the regions ω_R and ω_T where the dose $C_{\omega_R} y$ and $C_{\omega_T} y$ is *at least* that level (i.e., the objective is to minimize the area of the shaded regions between the dotted lines and the curves).

We first note that the solution of the regularized state-constrained problem, shown in Figure 1 for the final $\gamma \approx 1.22 \cdot 10^{-4}$, gives poor results. This is not unexpected: the problem (1.3) is clearly infeasible; we see that for all γ, we have $C_{\omega_T} y < U$ everywhere while $C_{\omega_R} y > L$ on around 13% of the risk region. This means that the primary design objective—exceeding the minimal dose U on ω_T—is not achieved at all.

Meanwhile, the solution to the regularized dose-penalized problem for $\tilde{\beta}_1 = \tilde{\beta}_2 = 10^3$ and final $\gamma \approx 2.38 \cdot 10^{-5}$ shown in Figure 2 is clearly superior: a significant portion (55%) of the target region ω_T has at least a dose of U, while the area where $C_{\omega_R} y > L$ is slightly smaller (11%). Increasing $\tilde{\beta}_1$ to 10^4 (see Figure 3, with final $\gamma \approx 1.87 \cdot 10^{-7}$) further improves the dose coverage on the tumor (87%), but does so at the expense of increased violation of the dose constraint on

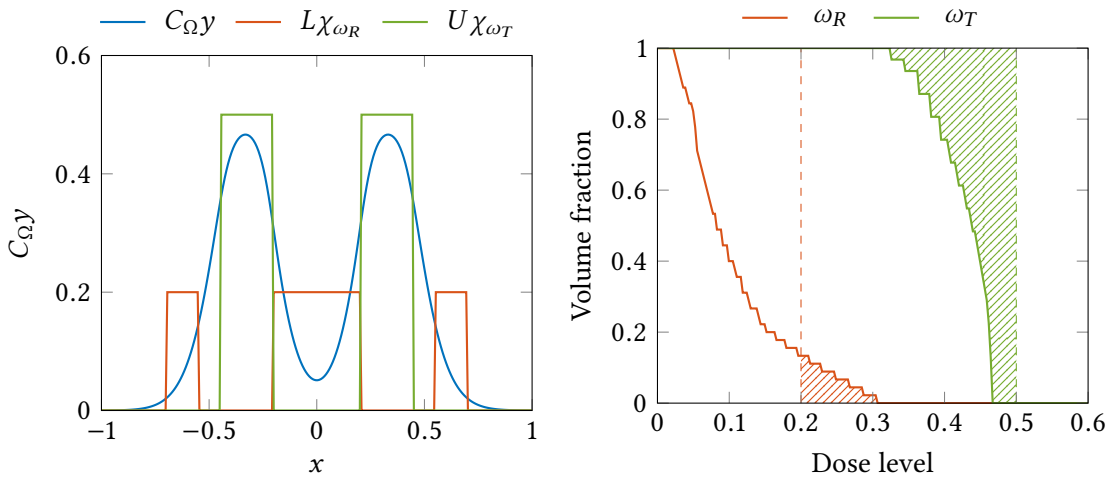

(a) Final dose $C_\Omega y$, risk level $L\chi_{\omega_R}$, target level $U\chi_{\omega_T}$ (b) Dose volume histogram for risk region ω_R and target region ω_T

Figure 1: Dose information for dose-constrained problem (1.3)

the risk region (22% instead of 11%). Conversely, increasing $\tilde{\beta}_2$ to 10^4 while keeping $\tilde{\beta}_1$ at 10^3 (see Figure 4, with final $\gamma \approx 4.77 \cdot 10^{-5}$) reduces the dose violation on the risk region to 2%, but the coverage on the tumor is now only 48%. Finally, increasing both $\tilde{\beta}_1$ and $\tilde{\beta}_2$ to 10^4 (see Figure 5, with final $\gamma \approx 1.86 \cdot 10^{-7}$) yields a dose coverage on the tumor of 84%, while the dose violation on the risk region is still only 11%. Thus, in contrast to state constraints, the penalization of the dose violation is able to balance the competing objectives.

This comparison is more evident in Table 1 and Table 2, where we report for selected values of γ the number of Newton steps needed as well as the fraction of the area of ω_T where the resulting $C_{\omega_T} y$ is below U and the fraction of the area of ω_R where the resulting $C_{\omega_R} y$ is above L. We see that for regularized state constraints, the regularization approach becomes significantly more difficult for even modestly small γ while failing to give reasonable performance. In comparison, significantly fewer Newton iterations are required for the dose penalty, and the solutions to (OS_γ) give better performance for each γ. (Here it should be pointed out that because the ratio β/γ enters into the Newton system, the values of γ are not directly comparable between the case of state constraints and of dose penalization.) It can also be seen that, at least in this configuration, putting more weight on the tumor region increases the difficulty of the problem significantly, while putting more or equal weight on the risk region requires fewer Newton iterations for each value of γ and leads to convergence of the Newton method for smaller values. Finally, we note that the dose violation remains the same for all $\gamma < 3 \cdot 10^{-5}$.

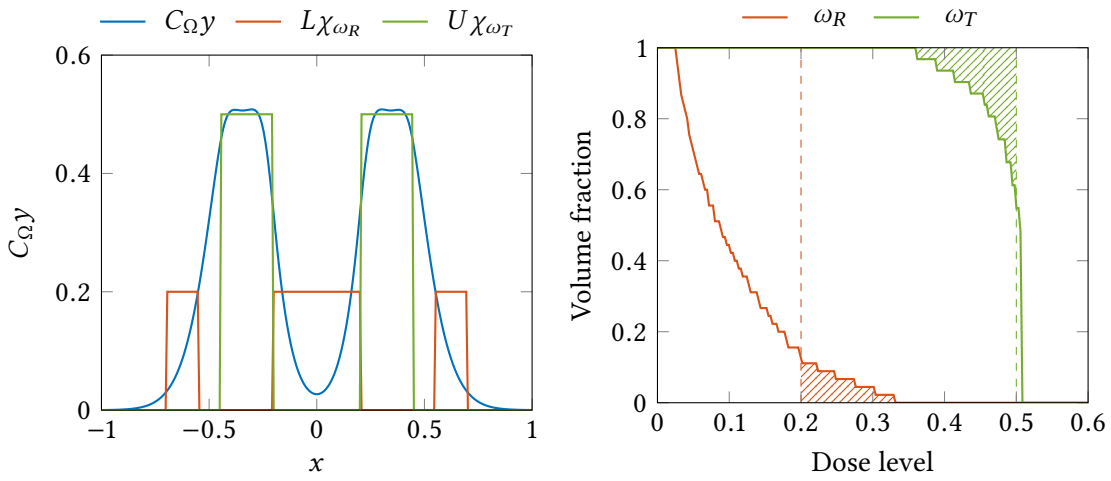

(a) Final dose $C_\Omega y$, risk level $L\chi_{\omega_R}$, target level $U\chi_{\omega_T}$ (b) Dose volume histogram for risk region ω_R and target region ω_T

Figure 2: Dose information for dose-penalized problem (1.1) with $\tilde{\beta}_1 = 10^3$, $\tilde{\beta}_2 = 10^3$

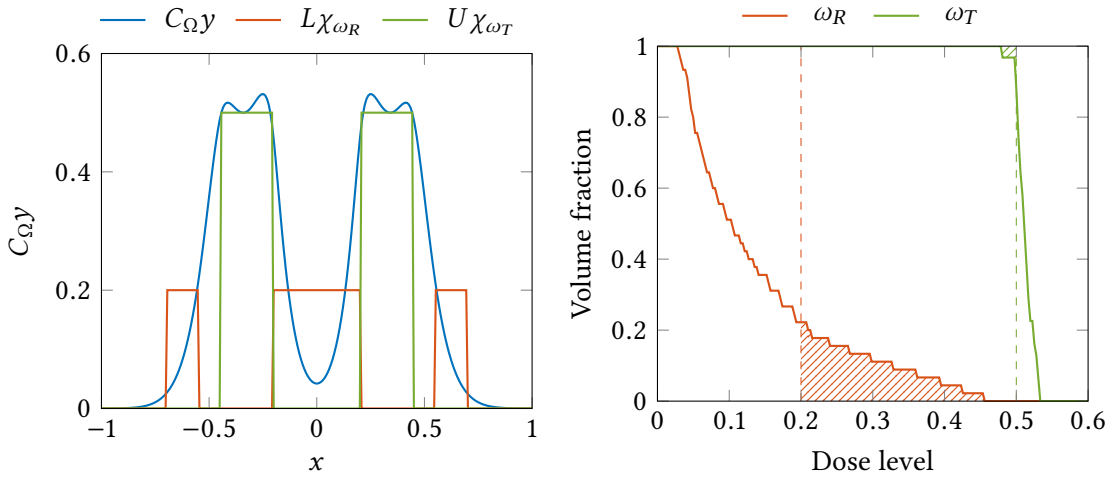

(a) Final dose $C_\Omega y$, risk level $L\chi_{\omega_R}$, target level $U\chi_{\omega_T}$ (b) Dose volume histogram for risk region ω_R and target region ω_T

Figure 3: Dose information for dose-penalized problem (1.1) with $\tilde{\beta}_1 = 10^4$, $\tilde{\beta}_2 = 10^3$

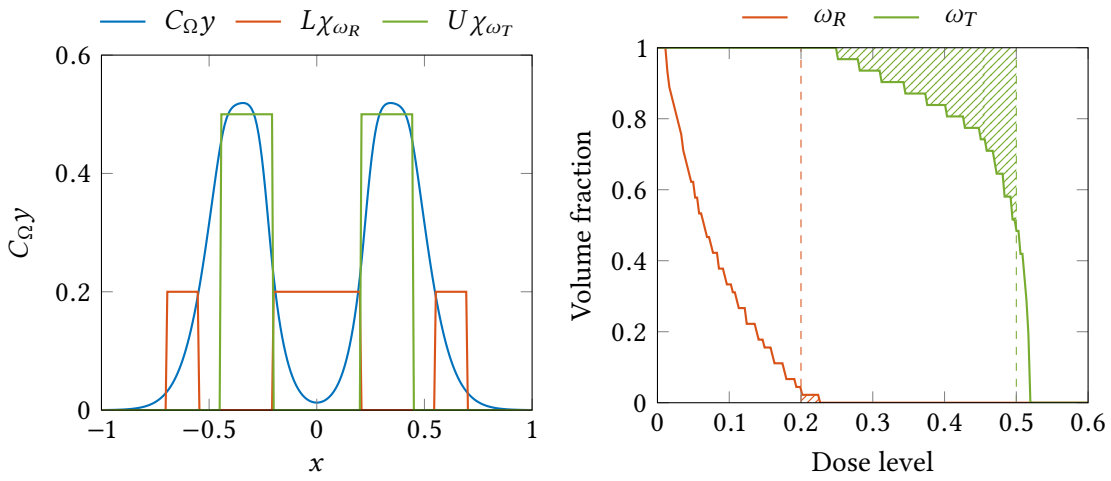

(a) Final dose $C_\Omega y$, risk level $L\chi_{\omega_R}$, target level $U\chi_{\omega_T}$ (b) Dose volume histogram for risk region ω_R and target region ω_T

Figure 4: Dose information for dose-penalized problem (1.1) with $\tilde{\beta}_1 = 10^3$, $\tilde{\beta}_2 = 10^4$

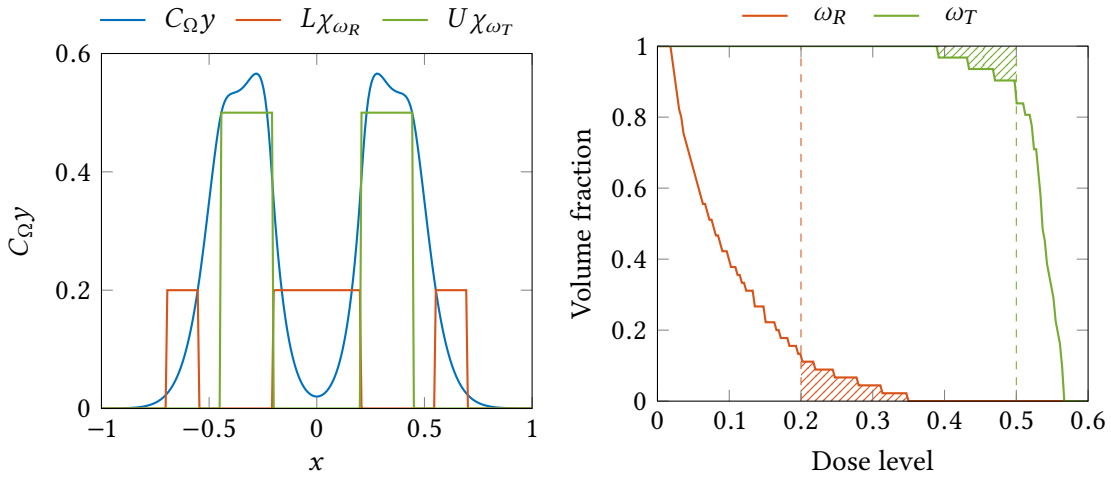

(a) Final dose $C_\Omega y$, risk level $L\chi_{\omega_R}$, target level $U\chi_{\omega_T}$ (b) Dose volume histogram for risk region ω_R and target region ω_T

Figure 5: Dose information for dose-penalized problem (1.1) with $\tilde{\beta}_1 = 10^4$, $\tilde{\beta}_2 = 10^4$

Table 1: Results for dose-constrained problem (1.3): number of SSN steps, volume fraction for risk and target regions for different values of γ ($*$ denotes failure to converge)

γ	$1.95 \cdot 10^{-1}$	$9.77 \cdot 10^{-4}$	$4.88 \cdot 10^{-4}$	$2.44 \cdot 10^{-4}$	$1.22 \cdot 10^{-4}$	$6.10 \cdot 10^{-5}$
#SSN	1	1	1	6	24	$*$
% ω_R above L	0	0	0.07	0.11	0.13	$*$
% ω_T below U	1	1	1	1	1	$*$

Table 2: Results for dose-penalized problem (1.1): number of SSN steps, volume fraction for risk and target regions for different values of γ ($*$ denotes failure to converge)

(a) $\tilde{\beta}_1 = 10^3$, $\tilde{\beta}_2 = 10^3$

γ	$4.88 \cdot 10^{-2}$	$3.05 \cdot 10^{-3}$	$4.77 \cdot 10^{-5}$	$2.38 \cdot 10^{-5}$	$1.19 \cdot 10^{-5}$	$1.86 \cdot 10^{-7}$
#SSN	2	4	2	1	$*$	$*$
% ω_R above L	0.13	0.13	0.11	0.11	$*$	$*$
% ω_T below U	1.00	0.45	0.45	0.45	$*$	$*$

(b) $\tilde{\beta}_1 = 10^4$, $\tilde{\beta}_2 = 10^3$

γ	$4.88 \cdot 10^{-2}$	$3.05 \cdot 10^{-3}$	$4.77 \cdot 10^{-5}$	$2.38 \cdot 10^{-5}$	$1.19 \cdot 10^{-5}$	$1.86 \cdot 10^{-7}$
#SSN	3	1	1	1	1	1
% ω_R above L	0.22	0.22	0.22	0.22	0.22	0.22
% ω_T below U	0.26	0.16	0.16	0.13	0.13	0.13

(c) $\tilde{\beta}_1 = 10^3$, $\tilde{\beta}_2 = 10^4$

γ	$4.88 \cdot 10^{-2}$	$3.05 \cdot 10^{-3}$	$4.77 \cdot 10^{-5}$	$2.38 \cdot 10^{-5}$	$1.19 \cdot 10^{-5}$	$1.86 \cdot 10^{-7}$
#SSN	3	3	4	$*$	$*$	$*$
% ω_R above L	0.04	0.02	0.02	$*$	$*$	$*$
% ω_T below U	0.62	0.52	0.52	$*$	$*$	$*$

(d) $\tilde{\beta}_1 = 10^4$, $\tilde{\beta}_2 = 10^4$

γ	$4.88 \cdot 10^{-2}$	$3.05 \cdot 10^{-3}$	$4.77 \cdot 10^{-5}$	$2.38 \cdot 10^{-5}$	$1.19 \cdot 10^{-5}$	$1.86 \cdot 10^{-7}$
#SSN	3	1	1	1	1	1
% ω_R above L	0.13	0.11	0.11	0.11	0.11	0.11
% ω_T below U	0.19	0.16	0.16	0.16	0.16	0.16

5 Conclusions

Volumetric dose constraints arising in, e.g., radiotherapy treatment planning can be formulated using L^1 penalization. This leads to a non-differentiable optimal control problem for partial differential equations that can be analyzed and shown to be well-posed using tools from convex analysis. After introducing a Moreau–Yosida regularization, these problems can be solved efficiently by a semismooth Newton method together with a homotopy in the regularization parameter. Our numerical examples illustrate that this approach significantly outperforms formulations via pointwise state constraints, in particular with respect to the dose volume histograms commonly used to evaluate structure survival probabilities.

Future work is concerned with the extension of the approach to radiative transport equations—which are challenging both analytically and numerically due to their hyperbolic nature and their increased dimensionality (angular dependence)—as well as the application to concrete problems in radiotherapy treatment planning.

References

[1] R. Barnard, M. Frank, and M. Herty. Optimal radiotherapy treatment planning using minimum entropy models. *Applied Mathematics and Computation*, 219(5):2668–2679, November 2012. doi:10.1016/j.amc.2012.08.099.

[2] H. H. Bauschke and P. L. Combettes. *Convex Analysis and Monotone Operator Theory in Hilbert Spaces*. Springer, New York, 2011. doi:10.1007/978-1-4419-9467-7.

[3] H. Brezis, M. G. Crandall, and A. Pazy. Perturbations of nonlinear maximal monotone sets in Banach space. *Communications on Pure and Applied Mathematics*, 23(1):123–144, 1970. doi:10.1002/cpa.3160230107.

[4] C. Clason, K. Ito, and K. Kunisch. A convex analysis approach to optimal controls with switching structure for partial differential equations. *ESAIM: Control, Optimisation and Calculus of Variations*, 22(2):581–609, 2016. doi:10.1051/cocv/2015017.

[5] C. Clason and B. Jin. A semismooth Newton method for nonlinear parameter identification problems with impulsive noise. *SIAM Journal on Imaging Sciences*, 5:505–538, 2012. doi:10.1137/110826187.

[6] C. Clason and K. Kunisch. Multi-bang control of elliptic systems. *Annales de l'Institut Henri Poincaré (C) Analyse Non Linéaire*, 31(6):1109–1130, 2014. doi:10.1016/j.anihpc.2013.08.005.

[7] C. Clason, A. Rund, K. Kunisch, and R. C. Barnard. A convex penalty for switching control of partial differential equations. *Systems & Control Letters*, 89:66–73, 2016. doi:10.1016/j.sysconle.2015.12.013.

[8] I. Ekeland and R. Témam. *Convex Analysis and Variational Problems*, volume 28 of *Classics Appl. Math.* SIAM, Philadelphia, 1999. doi:10.1137/1.9781611971088.

[9] M. Frank, M. Herty, and M. Hinze. Instantaneous closed loop control of the radiative transfer equations with applications in radiotherapy. *ZAMM Z. Angew. Math. Mech.*, 92(1):8–24, 2012. doi:10.1002/zamm.201000191.

[10] M. Frank, M. Herty, and A. N. Sandjo. Optimal radiotherapy treatment planning governed by kinetic equations. *Math. Models Methods Appl. Sci.*, 20(4):661–678, 2010. doi:10.1142/S0218202510004386.

[11] R. Herzog, G. Stadler, and G. Wachsmuth. Directional sparsity in optimal control of partial differential equations. *SIAM Journal on Control and Optimization*, 50(2):943–963, 2012. doi:10.1137/100815037.

[12] R. Herzog, G. Stadler, and G. Wachsmuth. Erratum: Directional sparsity in optimal control of partial differential equations. *SIAM Journal on Control and Optimization*, 53(4):2722–2723, 2015. doi:10.1137/15M102544X.

[13] J.-B. Hiriart-Urruty and C. Lemaréchal. *Fundamentals of Convex Analysis*. Springer-Verlag, Berlin, 2001. doi:10.1007/978-3-642-56468-0.

[14] K. Ito and K. Kunisch. Semi-smooth Newton methods for state-constrained optimal control problems. *Systems & Control Letters*, 50(3):221–228, 2003. doi:10.1016/S0167-6911(03)00156-7.

[15] K. Ito and K. Kunisch. *Lagrange Multiplier Approach to Variational Problems and Applications*. SIAM, Philadelphia, PA, 2008. doi:10.1137/1.9780898718614.

[16] T. Landberg, J. Chavaudra, J. Dobbs, G. Hanks, K.-A. Johansson, T. Möller, and J. Purdy. ICRU Report 50–Prescribing, recording and reporting photon beam therapy. *Journal of the ICRU*, os26(1):NP, 1993. doi:10.1093/jicru/os26.1.Report50.

[17] D. M. Shepard, M. C. Ferris, G. H. Olivera, and T. R. Mackie. Optimizing the delivery of radiation therapy to cancer patients. *SIAM Review*, 41(4):721–744, 1999. doi:10.1137/S0036144598342032.

[18] G. Stadler. Elliptic optimal control problems with L^1-control cost and applications for the placement of control devices. *Computational Optimization and Applications*, 44(2):159–181, 2009. doi:10.1007/s10589-007-9150-9.

[19] M. Treutwein and L. Bogner. Elektronenfelder in der klinischen Anwendung. *Strahlentherapie und Onkologie*, 183:454–458, 2007. doi:10.1007/s00066-007-1687-0.

[20] M. Ulbrich. *Semismooth Newton Methods for Variational Inequalities and Constrained Optimization Problems in Function Spaces*. SIAM, Philadelphia, PA, 2011. doi:10.1137/1.9781611970692.

[21] M. Zarepisheh, M. Shakourifar, G. Trigila, P. S. Ghomi, S. Couzens, A. Abebe, L. Noreña, W. Shang, S. B. Jiang, and Y. Zinchenko. A moment-based approach for DVH-guided radiotherapy treatment plan optimization. *Physics in Medicine and Biology*, 58(6):1869, 2013. doi:10.1088/0031-9155/58/6/1869.